Simultaneous Sensing of Refractive Index and Temperature With Supermode Interference

Jose A. Flores-Bravo, Ruben Fernández, Enrique Antonio Lopez, Joseba Zubia, Axel Schülzgen, Rodrigo Amezcua Correa, and Joel Villatoro

***Abstract*—In general, a sensor is used to monitor a single parameter only, and in many cases, a reference sensor is necessary to compensate the effect of temperature. Here, we demonstrate that a single supermode interferometer is capable of monitoring two parameters simultaneously. Said interferometer was fabricated with a segment of strongly coupled multicore fiber fusion spliced at the end of a standard single mode fiber. The free end of the multicore fiber was flat, thus, it behaved as a low reflectivity mirror whose reflection depended on the external refractive index. The reflection spectrum of our supermode interferometer consisted of well-defined periodic maxima and minima whose values and position varied when the interferometer was exposed to refractive index and temperature changes. In the Fourier domain, the changes of the interference pattern can be decoded easily. We demonstrate that the supermode interferometer here proposed can be useful to measure the thermo-optic coefficient of a sample. An important advantage of the device reported here is that the length of the multicore fiber is not determinant on the performance of the sensor. In addition, the device can be reused multiple times.**

***Index Terms*—Dual parameter sensors, interferometers, Multicore fiber sensors, optical fiber sensors, refractometers, supermode interferometers, thermo-optic coefficient.**

I. Introduction

OPTICAL fibers have an intrinsic temperature sensitivity which makes them good thermometers, but such sensitivity is an issue when one wants to measure or monitor the refractive index of a sample. In a laboratory environment, refractive index measurements can be carried out at constant temperature. However, for *in situ* refractive index measurements and in many other applications, temperature cannot be controlled. In such circumstances, it is necessary to measure simultaneously index and temperature.

To be a real alternative for practical applications, a fiber optic sensor that is capable of measuring refractive index and temperature simultaneously must fulfill some important requirements. Its fabrication must be easy and reproducible; it must be robust, easy to use and clean; the refractive index measuring range of the sensor must be as broad as possible, etc.

So far, the optical fiber sensing community has made substantial efforts to devise sensors that fulfill such requirements. In Ref. [1], for example, different sensor architectures that can be used to measure temperature and refractive index are reviewed. Several of such architectures include a reference sensor for which their fabrication may entail complex assembly procedures. The addition of a reference sensor may compromise the reproducibility, interrogation, and cost of a device.

To overcome the above issues, single fiber optic sensors capable of monitoring index and temperature have been proposed in the literature. These include long-period gratings [2], [3], Bragg gratings [4]–[10], single-cavity Fabry-Perot interferometers fabricated with polymer [11] or by fusion splicing [12], and metal-coated fibers [13], [14] among others. The main disadvantage of grating-based sensors is their poor sensitivity for refractive indices below 1.4 or their expensive interrogation. The drawbacks of sensors based on polymer- or metal-coated fiber include poor reproducibility or issues related with their reusability.

Single interferometers built with conventional [15]–[18], polarization-maintaining fibers [19], [20] or etched multicore fibers [21], [22] have also been proposed for simultaneous sensing of index and temperature. The inconvenience of such interferometers is the need of a multi-step fabrication process or complex interrogation and signal processing. Single-mode-multimode structures that operate in reflection [23]–[26] have been demonstrated for index and temperature measurements as well. The disadvantage in these cases is the lack of control on the number of modes that are excited in the segment of multimode fiber. Moreover, in Refs. [24]–[26] temperature and index were measured in separate experiments.

To make a mode interferometer functional and practical for dual parameter sensing it is important to control the modes that participate in the interference. In addition, the fabrication of the interferometer must include minimal steps to ensure reproducibility and low cost.

Manuscript received April 9, 2021; revised July 21, 2021 and August 27, 2021; accepted September 16, 2021. Date of publication September 20, 2021; date of current version November 16, 2021. This work was supported in part by the Ministerio de Economía y Competitividad (Spain) and the European Regional Development Fund under Grants PGC2018-101997-B-I00 and RTI2018-094669-B-C31, and in part by the Departamento de Educacion del Gobierno Vasco, under Grant IT933-16. *(Corresponding author: Joel Villatoro.)*

Jose A. Flores-Bravo, Ruben Fernández, and Joseba Zubia are with the Department of Communications Engineering, University of the Basque Country UPV/EHU, E-48013 Bilbao, Spain (e-mail: joseangel.flores@ehu.eus; ruben.fernandez@ehu.eus; joseba.zubia@ehu.eus).

Enrique Antonio Lopez, Axel Schülzgen, and Rodrigo Amezcua Correa are with the CREOL The College of Optics and Photonics, University of Central Florida, Orlando, FL 162700 USA (e-mail: jealopez@creol.ucf.edu; axel@creol.ucf.edu; r.amezcua@creol.ucf.edu).

Joel Villatoro is with the Department of Communications Engineering, University of the Basque Country UPV/EHU, E-48013 Bilbao, Spain; he is also with IKERBASQUE, Basque Foundation for Science, E-48011 Bilbao, Spain (e-mail: agustinjoel.villatoro@ehu.es).

Color versions of one or more figures in this article are available at https://doi.org/10.1109/JLT.2021.3113863.

Digital Object Identifier 10.1109/JLT.2021.3113863

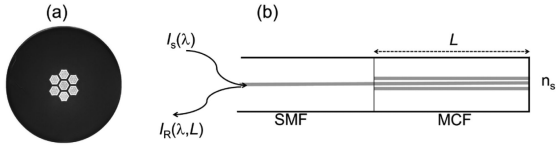

Fig. 1. (a) Cross section of the MCF used in the experiments. (b) Schematic representation of the supermode interferometer of length *L*. The profile of the excitation light source and the reflection spectrum of the interferometer are denoted as $I_{\rm s}(\lambda)$ and $I_{\rm R}(\lambda,L)$, respectively. The refractive index of the sample is denoted as $n_{\rm s}$.

Here, we propose a device that may fulfill the aforementioned requirements. We used an optical fiber designed to support specific interfering modes, which is called strongly-coupled multicore fiber (MCF). These fibers have opened up new alternatives to devise mode interferometers for sensing applications, see for example Refs. [27]–[29]. In the referred MCFs, the cores are close to each other to allow optical interaction among them. Strongly-coupled MCFs support several supermodes and can be treated as a special form of multimode fiber [30]. However, under specific excitation conditions it is possible to excite and recombine only two supermodes in the MCF [31].

Supermode interferometers are promising for optical fiber sensing due their distinct advantages. First, it is possible to have control on the supermodes that participate in the interference. Hence, the performance of a sensor can be predicted and even tailored. Second, they are compact and robust and can be fabricated by splicing a centimeter-long segment of such an MCF to SMF. Third, here is no need to use expensive fan-in and fan-out devices to interrogate a supermode interferometer. Moreover, the insertion losses of a SMF-MCF junction may be minimal if the SMF and the MCF have the same numerical aperture [27]–[29].

In this work, we demonstrate that a single supermode interferometer can be capable of monitoring temperature and refractive index simultaneously. Temperature is encoded in a shift of the interference pattern and refractive index in the visibility of the same pattern. To interrogate our devices, a narrow band light source and a low resolution spectrometer may be sufficient.

As an application, we demonstrate the use of our supermode interferometer to measure the thermo-optic coefficient of a liquid. However, many other applications are foreseen as in many sensing applications temperature cannot be constant and must be monitored along with the target parameter.

II. Theory of a Supermode Interferometer

The supermode interferometer used in our experiments was built with the MCF whose cross section is shown in Fig. 1(a). The MCF has seven coupled cores; all the cores are identical, one of them is in the geometrical center of the fiber and the other six cores are located around the central core. The numerical aperture of all the cores of the MCF is approximately equal to that of the SMF, which is 0.14 at 1550 nm.

The structure of the interferometer is shown schematically in Fig. 1(b). It consists of a piece of MCF of length *L* fusion spliced at the distal end of a conventional SMF. The MCF end was cleaved, in this manner; the MCF facet behaves as a reflector. Said reflector is sensitive to the refractive index of a sample that may be in direct contact with the MCF facet.

In the SMF-MCF structure shown in Fig. 1(b), the unique core of the SMF and the central core of the MCF are axially aligned and in physical contact. Thus, only the fundamental SMF mode excites the MCF. This assumption is valid in a range of wavelengths in which the SMF and the cores of the MCF are single mode, between 1260 and 1650 nm, approximately. Under these excitation conditions, only two supermodes that have nonzero intensity in the central core are excited in the MCF. This has been demonstrated experimentally and analytically, by other authors, see for example [27], [31].

The propagation constants of the two excited supermodes in the MCF can be denoted as β_1 and β_2. Both β_1 and β_2 depend mainly on the wavelength (λ) of the excitation light source, the size of the cores, their separation and the material the cores are made of. The light source, the geometry, and the refractive index (material) of the cores of the MCF can be chosen. Thus, with coupled-core MCF, it is possible to tailor the properties of a supermode interferometer. This is a distinctive advantage over their counterparts built with other optical fibers in which there is no control on the modes that interfere.

The difference in the propagation constants of the interfering supermodes can be expressed as $\Delta\beta = 2\pi\Delta n/\lambda$, where $\Delta n = n_{\rm e1} - n_{\rm e2}$, with $n_{\rm e1}$ and $n_{\rm e2}$ the effective refractive indices of the supermodes excited in the MCF. As the supermodes travel twice the segment of MCF, thus, the reflection of the SMF-MCF structure shown in Fig. 1(b) can be expressed as

$$I_{\rm R}\left(\lambda,\ L\right) = I_{\rm s}\left(\lambda\right) R_F \left[I_1 + I_2 + 2\sqrt{I_1 I_2}\cos\left(4\pi\Delta nL/\lambda\right)\right] \tag{1}$$

In Eq. (1), $I_{\rm s}(\lambda)$ denotes the profile of the light source, $R_{\rm F}$ is the Fresnel reflection coefficient that depends on the index of the sample ($n_{\rm s}$). I_1 and I_2 denote the intensities of the two supermodes that are excited in the MCF. Note that Eq. (1) describes an interference pattern that can be detected by means of the SMF connected to a spectrometer by means of a fiber coupler or circulator.

An interference pattern can be characterized by its visibility (*V*). In our case, *V* is the difference between the maximum and minimum of Eq. (1) divided by the sum of such maximum and minimum. This means, $V = 2\sqrt{\mathrm{I_1 I_2}}/(\mathrm{I_1}+\mathrm{I_2})$. Therefore, the normalized reflection spectrum of the structure shown in Fig. 1(b) can be expressed as:

$$R(\lambda,\ L)\ =\ I_{\rm ns}\left(\lambda\right) R_F \left[1 + V\cos\left(4\pi\Delta nL/\lambda\right)\right]/\left(1+V\right)] \tag{2}$$

In Eq. (2), $I_{\rm ns}(\lambda)$ is the normalized spectral distribution of the light source that excites the MCF. In a practical application, the excitation light source may be a narrow-band superluminescent diode (SLED), which has a quasi-Gaussian spectral distribution.

To calculate the reflection spectrum of the structure depicted in Fig. 1(b) it is necessary to know the wavelength dependence of Δn. To do so, a commercial simulation software (MODE from Lumerical) was used. In the simulations, a conventional SMF with a core of 8.2 μm in diameter and a numerical aperture of 0.14 was considered. The diameter of each core in the MCF was considered to be 11 μm and the separation between neighbor cores of 13 μm. The refractive index of each core in the MCF

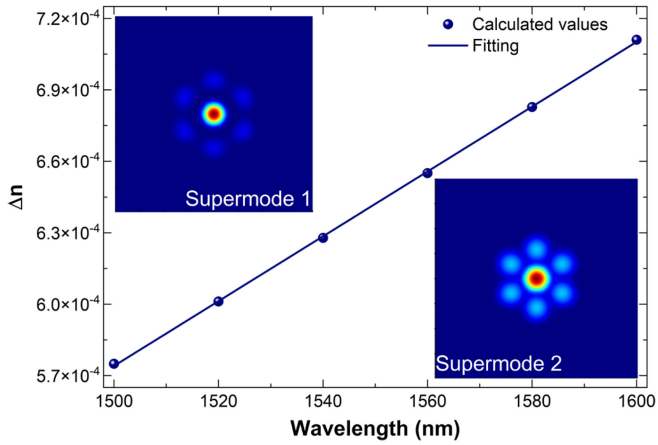

Fig. 2. Δn as a function of wavelength calculated of the MCF shown in Fig. 1(a). The inset images show the profiles at 1550 nm of the two excited supermodes in the MCF.

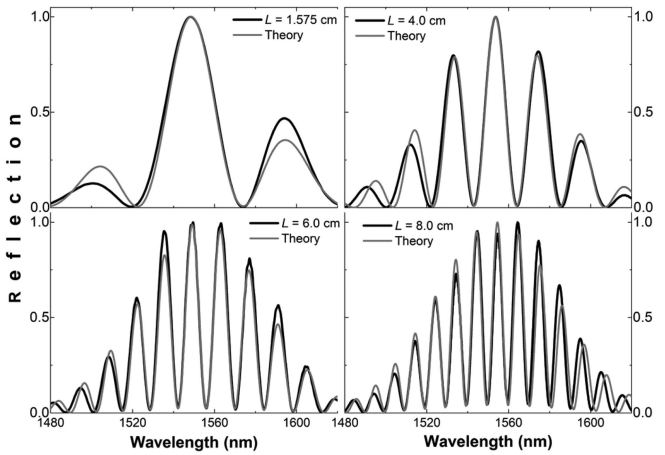

Fig. 3. Calculated (dotted lines) and measured (solid lines) reflection spectra of some supermode interferometers built with the MCF shown in Fig. 1(a). The values of L are indicated in the graphs.

was considered to be 1.451 and the index of MCF cladding of 1.444.

Fig. 2 shows the calculated values of Δn of the seven-coupled core fiber shown in Fig. 1(a) at discrete wavelengths. The profiles of the two supermodes that have nonzero intensity in the central core of the MCF are shown in the insets of Fig. 2. The simulations show that Δn depends linearly on the wavelength. Thus, the wavelength dependence of Δn can be expressed as:

$$\Delta n(\lambda) = a_7\lambda + b_7 \tag{3}$$

When λ is in nanometers, the following values were found for the MCF shown in Fig. 1(a): $a_7 = 1.3531 \times 10^{-6}$ and $b_7 = -1.4611 \times 10^{-3}$. Thus, to predict the reflection spectrum of a supermode interferometer built with different lengths of the MCF segment, we only need to substitute Eq. (3), with the values of a_7 and b_7 given above, in Eq. (2).

To verify the validity of our theoretical predictions and to confirm that the interference was between two supermodes only, we fabricated several samples and measured their reflection spectra. In Fig. 3 we show the theoretical and measured spectra of some samples where L was between 1.575 and 8 cm. In the theoretical spectrum, it was assumed that V was between 0.92 and 0.98. The light source used in the experiments was an SLED whose spectral profile was Gaussian, so it was expressed as $I_{\rm ns}(\lambda) = exp[-(\lambda-\lambda_0)^2/(2\Delta\lambda^2)]$, where λ_0 is the peak or central wavelength of the SLED and $\Delta\lambda$ the spectral width of the same. The SLED used in our experiments had the following values: $\lambda_0 \approx$1550 nm and $\Delta\lambda \approx 30$ nm.

It can be noted from Fig. 3 the good agreement between our theoretical predictions with the experimental results. The results shown in such a figure suggest that our supermode interferometer is almost ideal as the visibility of the interference pattern reaches values close to 1.

III. Refractive Index Sensing

Our supermode interferometers were characterized as refractive index sensors at a constant temperature. To do so, we used calibrated refractive index liquids from Cargille laboratories, which had nominal indices between 1.300 and 1.400 (at 589.3 nm and 25 °C). Two supermode interferometers were tested, one with $L = 4$ cm and the other with $L = 8$ cm. In each measurement, the flat MCF tips of both samples were cleaned in an ultrasonic cleaner that was filled with ethyl alcohol, dried with air, and then they were immersed in Cargille liquids with different refractive indices. It is important to point out that the MCF segments were straight during the measurements.

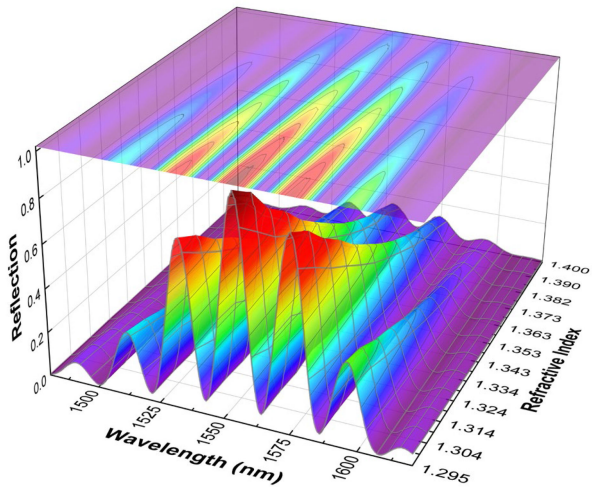

Fig. 4. Reflection spectra observed when the MCF tip of a supermode interferometer was immersed in different calibrated refractive indices. In all cases, $L = 4$ cm. The top graph is a projection of the 3D spectra.

The MCF interferometer and the calibrated refractive index liquids were inside an oven whose temperature was 25 ± 0.5 °C. To ensure that the liquids and the supermode interferometers reached thermal stability, we waited 5 minutes before collecting the reflection spectra.

In Fig. 4, we show the reflection spectra observed when the 4 cm-long interferometer was immersed in the aforementioned liquids. It was observed that the reflection spectrum decreased as the index of the liquid increased. This behavior is due to changes

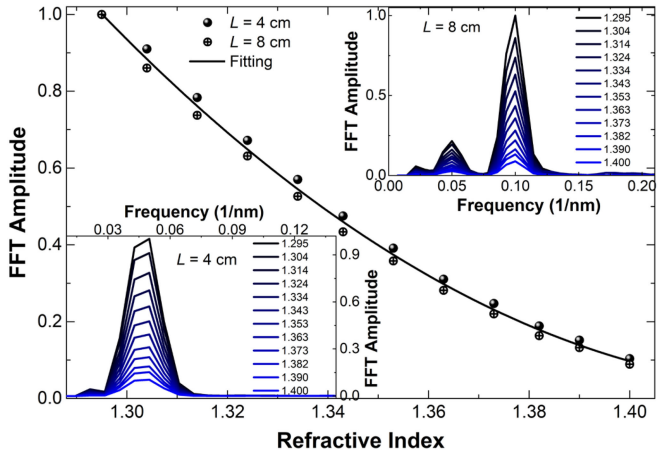

Fig. 5. Calibration curve showing the FFT amplitude as a function of the refractive index. The lengths of the interferometers are indicated. The continuous line is a fitting to the average data obtained with devices with $L = 4$ and $L = 8$ cm. The inset graphs show the FFT amplitudes at different indices.

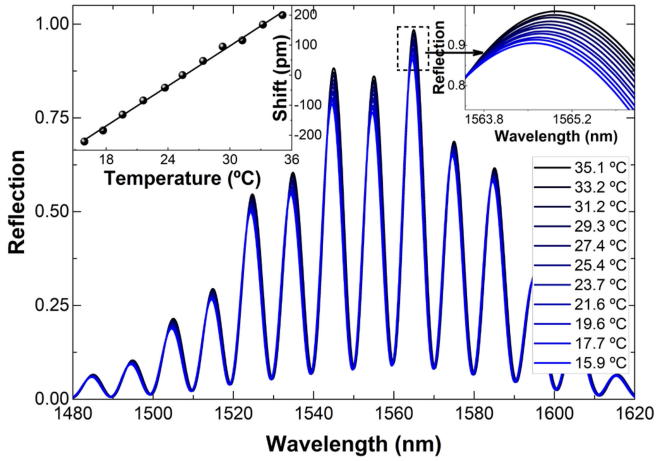

Fig. 6. Reflection spectra observed when a supermode interferometer fabricated with 8 cm of MCF was immersed in a liquid with index of 1.2945 (at 1550 nm) and the temperature was changed between 15.9 and 35.1 °C. The inset graphs show the shift caused by temperature. At 25 °C the shift was considered to be 0. A zoom in of a maximum of the spectra is also shown.

in the reflectivity of the MCF-sample interface that affect the intensity of the two interfering supermodes, and consequently, the interference pattern.

As the temperature is constant the interference patterns should not shift. The calculated shift was found to be ca. 50 pm, but we attribute that it is due to the errors in finding the wavelength position of the peaks of the interference pattern, particularly when the index gets closer to that of glass. For example, when $n_s = 1.40$, the reflection from the MCF-liquid interface is 0.032%, which is ten times lower than the reflectivity when $n_s = 1.30$.

The experiments were also carried out with the 8 cm-long supermode interferometer. Similar behavior than that of the 4-long interferometer was observed (graphs not shown).

There are different manners to correlate the changes of the reflection spectra shown in Fig. 4 with the refractive index in which the MCF facet was immersed to. In our case, the fast Fourier transform (FFT) of each spectrum was calculated. The calculation of the FFT of an interference pattern is straightforward. The FFT has been used for several authors to decode the parameters that perturb an interferometic sensor, see for example Refs. [29], [32]–[34]. In our case, the height of the FFT amplitude was correlated with the index of the sample.

Fig. 5 displays the FFT amplitude as a function of the index of the liquids observed with the 4- and 8-cm long supermode interferometers. The inset graphs show the normalized FFT amplitudes for different indices of the liquids. For convenience, the FFT amplitude was considered as 1 when $n_s = 1.3000$.

It can be concluded from the results shown in Fig. 5 that a short or a long interferometer can provide similar calibration curves. This suggests that the length of the MCF may not be crucial on the performance of a supermode interferometer if it is used as refractive index sensor. Hence, if compactness is important, a short segment of MCF can be used to fabricate the sensor.

The calibration curves that were obtained for the short and long interferometers were fitted with the following expression:

$$n_s = a + b_1 A_F + b_2 {A_F}^2 \quad (4)$$

In Eq. (4), n_s is the refractive index of the sample; a, b_1, and b_2 are fitting values, and A_F is the amplitude of the FFT which is measured experimentally. The fitting values a, b_1, and b_2 can be obtained for each sensor when it is calibrated.

In different situations, the temperature cannot be controlled during the index measurements. Thus, we carried out experiments in which the temperature changed in a controlled manner. To do so, we immersed the MCF end of the 8 cm-long interferometer in a liquid with nominal index of 1.300. The whole MCF segment and the liquid were exposed to temperatures between 15 and 35 °C. The reason of this temperature range was because Cargille laboratories provide (in the datasheet) the refractive index of the referred liquid in a such a range of temperatures.

The results of the experiments mentioned in the above paragraph are summarized in Fig. 6. The figure shows that the interference pattern shifts (22 pm per degree Celsius) and that the amplitude of the same pattern changes. The shift of the interference pattern is due to changes of Δn of the supermodes as they are sensitive to temperature as demonstrated in Ref. [27]. The changes in the amplitude are due to alterations of the refractive index of the sample that affect the reflectivity of the MCF-liquid interface.

The measured refractive indices at different temperatures are shown in Fig. 7. It should be pointed out that the indices were calculated with Eq. (4) with the following coefficients $a = 1.4131$, $b_1 = -0.17962$, and $b_2 = 0.06199$ that were obtained from the calibration curve of the 8 cm long MCF interferometer. It was assumed that $n_s = 1.295$ at 1550 nm and 25 °C. From the fitting of the experimental points of Fig. 7, we obtained the thermo-optic coefficient (TOC) of the referred liquid. The TOC we found experimentally was -2.75×10^{-4} °C^{-1}, which differs ca. 18% with the value (-3.33×10^{-4} °C^{-1}) provided by Cargille laboratories. It is important to mention that the referred laboratories provide TOCs of their liquids at 589 nm. In our case, we considered that the peak or central wavelength of the SLED use in our experiments was 1550 nm.

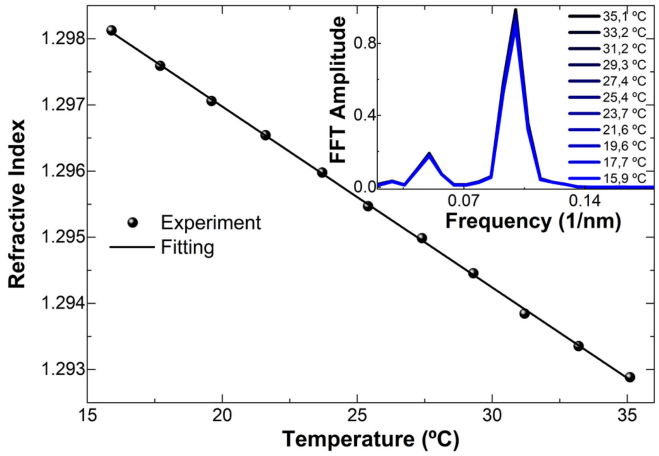

Fig. 7. Refractive index as a function of temperature calculated from the spectra shown in Fig. 6. The inset graph show the FFT amplitude at different temperatures.

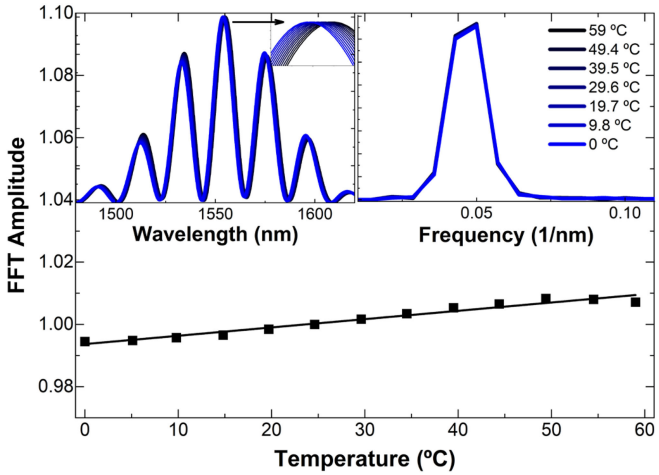

Fig. 8. Amplitude of the FFT as a function of temperature observed when n_s was 1 (air). The normalized reflection spectra and FFT amplitudes at different temperatures are shown in the insets. In all cases L was 4 cm.

To investigate the temperature-index crosstalk of our interferometers we analyzed their response to temperature when the external medium was air. To do this investigation, the facet of the MCF was protected and the interferometer was exposed to temperatures from 0 to 60 °C. The normalized spectra and FFT amplitude at different temperatures are shown in the insets of Fig. 8. In said graph, we also show the FFT amplitude as a function of temperature. At 25 °C, the FFT amplitude was considered to be 1.

From Fig. 8, the calculated temperature sensitivity of the interferometer was found to be 22.86 pm/°C, which is similar to the sensitivity when the MCF was in contact with a fluid. This suggests that a liquid in contact with the MCF facet does not affect the temperature sensitivity of the interferometer. From the results shown in Fig. 8, we also calculated the fluctuations of the FFT amplitude in the 15–35 °C temperature range. They were found to be ±0.198% with respect to the value of the FFT amplitude at 25 °C. These fluctuations induce errors in the measurements of the TOC. Thus, by considering such fluctuations, the TOC of the fluid referred above was found to be -3.29×10^{-4} °C^{-1} which agrees better with the value given by Cargille laboratories.

IV. Discussion

So far, several research groups have reported different optical fiber sensors with the aim of measuring refractive index and temperature simultaneously. However, in most cases, this is achieved with two sensors, one of them is used a as reference. Fabry-Perot interferometers (FPIs) with two cavities [35]–[38] or modal interferometers combined with other sensing elements [39]–[41] represent some examples. The main inconvenience of double-cavity FPIs include complex fabrication, as it is important to ensure multiple flat and parallel reflecting surfaces that are separated a microscopic distance.

Another approach to measure temperature and refractive index is by means of monitoring Fresnel reflections but in these cases, complex systems to compensate optical power fluctuations are necessary [34], [42]–[44].

The device reported here can provide data of temperature and refractive index of a sample without the need of a second sensor or a reference. This was achieved thanks to the well-defined sinusoidal interference patterns, which are due the beating of two supermodes in the MCF.

A comparison of the performance of the device here proposed with others reported in the literature is provided in Table I. It is important to clarify that the comparison was made only with sensors based on a single platform, grating, or interferometer. Index-temperature sensors that need a reference, two platforms, multiple gratings, dual cavities, or two interferometers belong to a different category and are reviewed in Ref. [1].

It is important to mention that a common drawback of the majority of refractive index sensors reported so far may be related to their cleaning. A refractive index sensor must be properly cleaned before and after its use to ensure reproducible results. Cleaning agents commonly used to clean the prism of commercial refractometers or optical fibers may be too aggressive to clean some sensors. For example, a nanometer thick metal layer cannot be cleaned easily. That is the reason sensors based on surface plasmon resonance are disposable. The cavity of some FPIs is made of polymer that cannot be polished or immersed in solvents. Changes in the dimensions or shape of the cavity of a FPI can severely affect its performance as index sensors.

The sensitive section of the sensors demonstrated here is the facet of an MCF. In our experiments, the MCF facet was cleaned with ethyl alcohol in an ultrasonic cleaner during 20 seconds before each measurement. The MCF facet can also be polished with a conventional optical fiber polisher. The effect of polishing on our devices may be a minute change in the length of the MCF segment. As demonstrated in Fig. 5, the length of the MCF has no effect on the measurement of the refractive index of a sample. The only important thing is to ensure a flat MCF end. Therefore, the sensors reported in this work can be reused multiple times.

It was found that refractive index induced errors of around 50 pm in finding the interference pattern shift; while temperature

TABLE I
COMPARISON OF REFRACTIVE INDEX (RI) AND TEMPERATURE (T) SENSORS BASED ON A SINGLE PLATFORM

Method or Technique	Measuring RI Range	Simultaneous RI and T	Reproducibility	References
Long period gratings	1.32 to 1.44	NO	LOW	2, 3
Fiber Bragg gratings	1.30 to 1. 45	YES in Ref. 9	HIGH	4-10
Surface plasmon resonance	1.33 to 1.38	YES	LOW	13-14
Fabry-Perot Interferometry	1 to 1.44	YES	LOW	11, 12
In-transmission multimode interference	1.33 to 1.40	NO	MODERATE	15-22
In-reflection multimode interference	1.33 to 1.38	YES in Ref. 23, NO in others	MODERATE	23-26
Supermode interference	1.29 to 1.40	YES	HIGH	**This work**

induced errors of around 0.2% in finding the amplitude of the FFT. We believe that the cross refractive-index-temperature sensitivity can be further reduced, for example, by means of a better processing of the interference patterns. The use of filters to calculate the FFT may help to improve the accuracy in finding its height.

V. CONCLUSION

In this work, we have demonstrated, for the first time to the best of our knowledge, the use of a single supermode interferometer for sensing two parameters (refractive index and temperature) simultaneously. One parameter is encoded in a shift of the interference pattern and the other in the amplitude of the same. The fabrication of the supermode interferometer is simple and reproducible. It consists of fusion splicing a segment of coupled core optical fiber to a conventional single mode fiber. The multicore fiber was cleaved to have a flat end that functioned as a low reflectivity mirror. Higher reflectivity can be achieved with metal or dielectric films deposited on the MCF facet.

Batch fabrication of the devices here proposed seems possible with commercially available fiber polishing or cleaving machines as the MCF is made of glass.

The MCF facet can be coated with a film that be sensitive to a gas or chemical parameter, thus, the supermode interferometer reported here can be used for gas or chemical sensing applications. The main advantage for such applications is that temperature and the target parameter can be monitored simultaneously.

REFERENCES

[1] S. Pevec and D. Donlagić, "Multiparameter fiber-optic sensors: A review," *Opt. Eng.*, vol. 58, no. 7, 2019, Art. no. 072009.

[2] T. Zhu, Y. J. Rao, and Q. J. Mo, "Simultaneous measurement of refractive index and temperature using a single ultralong-period fiber grating," *IEEE Photon. Technol. Lett.*, vol. 17, no. 12, pp. 2700–2702, Dec. 2005.

[3] S. Zhang *et al.*, "Few-mode fiber-embedded long-period fiber grating for simultaneous measurement of refractive index and temperature," *Appl. Opt.*, vol. 59, no. 29, pp. 9248–9253, 2020.

[4] X. Shu *et al.*, "Sampled fiber bragg grating for simultaneous refractive-index and temperature measurement," *Opt. Lett.*, vol. 26, no. 11, pp. 774–776, 2001.

[5] X. Chen *et al.*, "Simultaneous measurement of temperature and external refractive index by use of a hybrid grating in D fiber with enhanced sensitivity by HF etching," *Appl. Opt.*, vol. 44, no. 2, pp. 178–182, 2005.

[6] C. L. Zhao, X. Yang, M. S. Demokan, and W. Jin, "Simultaneous temperature and refractive index measurements using a 3° slanted multimode fiber Bragg grating," *J. Lightw. Technol.*, vol. 24, no. 2, pp. 879–883, Feb. 2006.

[7] H. Meng *et al.*, "Fiber Bragg grating-based fiber sensor for simultaneous measurement of refractive index and temperature," *Sensors Actuators, B: Chem.*, vol. 150, no. 1, pp. 226–229, 2010.

[8] Z. Chen *et al.*, "Side polished fiber Bragg grating sensor for simultaneous measurement of refractive index and temperature," in *Proc. SPIE*, vol. 7753, 2011, Art. no. 77538K.

[9] M. Yang, D. N. Wang, and C. R. Liao, "Fiber Bragg grating with microholes for simultaneous and independent refractive index and temperature sensing," *IEEE Photon. Technol. Lett.*, vol. 23, no. 20, pp. 1511–1513, Oct. 2011.

[10] H. Z. Yang *et al.*, "Cladless few mode fiber grating sensor for simultaneous refractive index and temperature measurement," *Sensors Actuators, A: Phys.*, vol. 228, pp. 62–68, 2015.

[11] X. L. Tan, Y. F. Geng, X. J. Li, Y. L. Deng, Z. Yin, and R. Gao, "UV-Curable polymer microhemisphere-based fiber-optic Fabry-Perot interferometer for simultaneous measurement of refractive index and temperature," *IEEE Photon. J.*, vol. 6, no. 4, Aug. 2014, Art. no. 7800208.

[12] T. Wang and M. Wang, "Fabry–Pérot fiber sensor for simultaneous measurement of refractive index and temperature based on an in-fiber ellipsoidal cavity," *IEEE Photon. Technol. Lett.*, vol. 24, no. 19, pp. 1733–1736, Oct. 2012.

[13] S. Weng, L. Pei, C. Liu, J. Wang, J. Li, and T. Ning, "Double-Side polished fiber SPR sensor for simultaneous temperature and refractive index measurement," *IEEE Photon. Technol. Lett.*, vol. 28, no. 18, pp. 1916–1919, Sep. 2016.

[14] J. S. Velázquez-González *et al.*, "Simultaneous measurement of refractive index and temperature using a SPR-based fiber optic sensor," *Sensors Actuators, B: Chem.*, vol. 242, pp. 912–920, 2017.

[15] J. Zhang *et al.*, "Simultaneous measurement of refractive index and temperature using a Michelson fiber interferometer with a hi-bi fiber probe," *IEEE Sensors J.*, vol. 13, no. 6, pp. 2061–2065, Jun. 2013.

[16] R. Xiong *et al.*, "Simultaneous measurement of refractive index and temperature based on modal interference," *IEEE Sensors J.*, vol. 14, no. 8, pp. 2524–2528, Aug. 2014.

[17] L. Zhang, D. Wang, J. Liu, and H. F. Chen, "Simultaneous refractive index and temperature sensing with precise sensing location," *IEEE Photon. Technol. Lett.*, vol. 28, no. 8, pp. 891–894, Apr. 2016.

[18] F. Yu, P. Xue, X. Zhao, and J. Zheng, "Simultaneous measurement of refractive index and temperature based on a peanut-shape structure in-line Fiber Mach-Zehnder interferometer," *IEEE Sensors J.*, vol. 19, no. 3, pp. 950–955, Feb. 2019.

[19] H.-J. Kim and Y.-G. Han, "Polarization-dependent in-line Mach–Zehnder interferometer for discrimination of temperature and ambient index sensitivities," *J. Lightw. Technol.*, vol. 30, no. 8, pp. 1037–1041, Apr. 2011.

[20] R.-A. Zhao *et al.*, "Polarization-maintaining fiber sensor for simultaneous measurement of the temperature and refractive index," *Opt. Eng.*, vol. 56, no. 5, 2017, Art. no. 057113.

[21] Y. Jiang *et al.*, "Simultaneous measurement of refractive index and temperature with high sensitivity based on a multipath fiber Mach–Zehnder interferometer," *Appl. Opt.*, vol. 58, no. 15, pp. 4085–4090, 2019.

[22] F. Mumtaz, Y. Dai, and M. A. Ashraf, "Inter-cross de-modulated refractive index and temperature sensor by an etched multi-core fiber of a MZI structure," *J. Lightw. Technol.*, vol. 38, no. 24, pp. 6948–6953, Dec. 2020.

[23] Y. H. Kim *et al.*, "Thermo-optic coefficient measurement of liquids based on simultaneous temperature and refractive index sensing capability of a two-mode fiber interferometric probe," *Opt. Exp.*, vol. 20, no. 21, pp. 23744–23754, 2012.
[24] S. Musa *et al.*, "Double-clad fiber Michelson interferometer for measurement of temperature and refractive index," *Microw. Opt. Technol. Lett.*, vol. 60, no. 4, pp. 822–827, 2018.
[25] H. Xue, H. Meng, W. Wang, R. Xiong, Q. Yao, and B. Huang, "Single-mode-multimode fiber structure based sensor for simultaneous measurement of refractive index and temperature," *IEEE Sensors J.*, vol. 13, no. 11, pp. 4220–4223, Nov. 2013.
[26] Y. Zhao, L. Cai, and X.-G. Li, "High sensitive modal interferometer for temperature and refractive index measurement," *IEEE Photon. Technol. Lett.*, vol. 27, no. 12, pp. 1341–1344, Jun. 2015.
[27] J. E. Antonio-Lopez *et al.*, "Multicore fiber sensor for high-temperature applications up to 1000 °C," *Opt. Lett.*, vol. 39, no. 15, pp. 4309–4312, 2014/08/01, 2014.
[28] J. Villatoro *et al.*, "Miniature multicore optical fiber vibration sensor," *Opt. Lett.*, vol. 42, no. 10, pp. 2022–2025, 2017.
[29] M. C. Alonso-Murias *et al.*, "Long-range multicore optical fiber displacement sensor," *Opt. Lett.*, vol. 46, no. 9, pp. 2224–2227, May 2021.
[30] K. Saitoh and S. Matsuo, "Multicore fiber technology," *J. Lightw. Technol.*, vol. 34, no. 1, pp. 55–66, Jan. 2016.
[31] N. Kishi, E. Yamashita, and K. Atsuki, "Modal and coupling field analysis of optical fibers with circularly distributed multiple cores and a central core," *J. Lightw. Technol.*, vol. 4, no. 8, pp. 991–996, Aug. 1986.
[32] H. Y. Choi *et al.*, "Cross-talk free and ultra-compact fiber optic sensor for simultaneous measurement of temperature and refractive index," *Opt. Exp.*, vol. 18, no. 1, pp. 141–149, Jan. 2010.
[33] S. Rota-Rodrigo, A. López-Aldaba, R. A. Pérez-Herrera, M. del Carmen López Bautista, Ó. Esteban, and M. López-Amo, "Simultaneous measurement of humidity and vibration based on a microwire sensor system using fast Fourier transform technique," *J. Lightw. Technol.*, vol. 34, no. 19, pp. 4525–4530, Oct. 2016.
[34] N. Cuando-Espitia, M. A. Fuentes-fuentes, D. A. May-Arrioja, I. Hernandez-Romano, R. M. Manuel, and M. Torres-Cisneros, "Dual-point refractive index measurements using coupled seven-core fibers," *J. Lightw. Technol.*, vol. 39, no. 1, pp. 310–319, Jan. 2021.
[35] T. Wang and M. Wang, "Fabry-Pérot fiber sensor for simultaneous measurement of refractive index and temperature based on an in-fiber ellipsoidal cavity," *IEEE Photon. Technol. Lett.*, vol. 24, no. 19, pp. 1733–1736, Oct. 2012.
[36] H. Sun *et al.*, "A hybrid fiber interferometer for simultaneous refractive index and temperature measurements based on Fabry-Perot/Michelson interference," *IEEE Sensors J.*, vol. 13, no. 5, pp. 2039–2044, May 2013.
[37] R. M. André *et al.*, "Simultaneous measurement of temperature and refractive index using focused ion beam milled Fabry-Perot cavities in optical fiber micro-tips," *Opt. Exp.*, vol. 24, no. 13, pp. 14053–14065, 2016.
[38] C. Zhou, Q. Zhou, C. He, J. Tian, Y. Sun, and Y. Yao, "Fiber optic sensor for simultaneous measurement of refractive index and temperature based on internal-and- external-cavity Fabry-Pérot interferometer configuration," *IEEE Sensors J.*, vol. 21, no. 8, pp. 9877–9884, Apr. 2021.
[39] C. Gouveia *et al.*, "Simultaneous measurement of refractive index and temperature using multimode interference inside a high birefringence fiber loop mirror," *Sensors Actuators, B: Chem.*, vol. 177, pp. 717–723, 2013.
[40] R. Oliveira *et al.*, "Simultaneous measurement of strain, temperature and refractive index based on multimode interference, fiber tapering and fiber Bragg gratings," *Meas. Sci. Technol.*, vol. 27, no. 7, 2016, Art. no. 075107.
[41] Y. Zhang *et al.*, "Simultaneous measurement of temperature and refractive index based on a hybrid surface plasmon resonance multimode interference fiber sensor," *Appl. Opt.*, vol. 59, no. 4, pp. 1225–1229, 2020.
[42] J. R. Zhao, X. G. Huang, and J. H. Chen, "A Fresnel-reflection-based fiber sensor for simultaneous measurement of liquid concentration and temperature," *J. Appl. Phys.*, vol. 106, no. 8, 2009, Art. no. 083103.
[43] H. Y. Choi *et al.*, "Cross-talk free and ultra-compact fiber optic sensor for simultaneous measurement of temperature and refractive index," *Opt. Exp.*, vol. 18, no. 1, pp. 141–149, 2010.
[44] R. Martinez-Manuel *et al.*, "Multi-point fiber refractometer using Fresnel reflection and a coherent optical frequency-domain multiplexing technique," *Appl. Opt.*, vol. 58, no. 3, pp. 684–689, Jan. 2019.